Optimization Study of Syngas Production from Catalytic Air Gasification of Rice Husk

Adrian Chun Minh Loy[a,b,1], Suzana Yusup[a,b,2], Bing Shen How[c], Yi Herng Chan[a,b,3],
Bridgid Lai Fui Chin[d], Azry Borhan[a,b,4], Huei Yeong Lim[a,b,5]

[a] Department of Chemical Engineering, Universiti Teknologi PETRONAS, 32610 Bandar Seri Iskandar, Perak, Malaysia

[b] Biomass Processing Lab, Centre for Biofuel and Biochemical Research (CBBR), Institute of Sustainable Living, Universiti Teknologi PETRONAS, 32610 Bandar Seri Iskandar, Perak, Malaysia
E-mail: [1]adrianminh@gmail.com; [2]drsuzana_yusuf@utp.edu.my; [3]kelvinyiherng@gmail.com; [4]azrybo@utp.edu.my; [5]limhueiyeong@gmail.com

[c] Department of Chemical Engineering, Faculty of Engineering, Computing and Science, Swinburne University of Technology
Jalan Simpang Tiga, 93350 Kuching, Sarawak, Malaysia
E-mail: bingshen.how@gmail.com

[d] Department of Chemical Engineering, Faculty of Engineering and Science, Curtin University Malaysia, CDT 250, 98009 Miri, Sarawak, Malaysia
Email: bridgidchin@curtin.edu.my

Abstract— Catalytic air gasification of rice husk was investigated in this study to optimize the hydrogen and syngas composition using a thermogravimetric analyzer coupled with a mass spectrometer. Then, a fixed bed reactor is used as a pilot plant to evaluate the practicality of the optimum parameters obtained from thermogravimetric analyzer test for upscaling. The catalyst used is coal bottom ash selected based on a previous study and obtained from a local power plant. The results from thermogravimetric analyzer test had shown that the optimum input parameters for syngas composition were at a reaction temperature of 900 °C, rice husk particle size of 250 µm, amounts of catalyst of 10 wt%, and air to biomass ratio of 1.25 to obtain product gas with 73.8 vol% of syngas composition. From a fixed bed reactor, 76.2 vol% of syngas composition is obtained, 3.25% higher than the previous test. Furthermore, 84.1 wt% of gaseous product yield, included syngas and CH_4, was obtained in the catalytic air gasification using a coal bottom ash catalyst. This showed the potential of coal bottom ash as the substitute for commercial catalysts in catalytic gasification. Lastly, principle component analysis was applied to evaluate the effect of temperature, particle size, air to biomass ratio, and coal bottom ash loading on H_2 and syngas production. H_2 production appears to be highly sensitive to the reaction temperature. Meanwhile, particle size, air to biomass ratio and catalyst loading were having a positive correlation with CO_2 and CH_4 but negative correlation with H_2.

Keywords— catalytic air gasification; optimization; syngas production.

I. INTRODUCTION

Renewable energy has been receiving considerable attention worldwide as the alternative means of energy resources in response to the mitigation of global energy crisis and sustainability issues, which revolve around the depletion of non-renewable energy sources and the environmental impacts associated with their utilization. One example of the environmental crisis is the greenhouse effect caused by the enormous CO_2 releases by the usage of fossil fuels for energy for more than half a century. The gradual shift from heavy dependency on fossil-based energy sources to increasingly established renewable energy technologies is happening over the past two decades [1]. In this context, various initiatives such as the enforcement of government policies and the provision of incentive schemes in promoting green energies have been implemented in order for renewable energy to penetrate the current energy production

technologies [2]. In general, renewable energy refers to the generation of a non-polluting and sustainable form of energy from natural environmental cycles, such as wind, solar, geothermal, hydropower, nuclear and biomass [3]. Among these renewable energy sources, biomass provides many prospects for conversion to various forms of products, such as biofuels for heat and power generation (bioenergy) and value-added bio-based chemicals [4], [5].

Gasification is one of the biomass thermochemical conversion technologies primarily employed for the generation of gaseous fuels [6]. Many studies had commonly used oxygen and steam as the gasifying agent working under high-temperature gasification mode. This is due to short residence time gives high carbon conversion associated with low tar production. However, the gasifier may be vulnerable to corrosion by the slag and if not handled properly, it can cause smelt-water explosions [7]. Thus, air gasification is a better option since it simplifies the gasification process and reducing the costs for operation and maintenance activities, as it is more complex and expensive to attain oxygen via air separation On the other hand, nitrogen content remains inert in the resultant gas for air gasification, where the calorific value is reduced due to dilution of the fuel gas [8].

Rice husk (RH) is produced as a biomass waste during the grain milling process to separate the husk with 700.7 million tons of annual global production capacity [9]. This has provided excellent prospects for its conversion to various types of fuels and products via thermochemical processes. Studies on gasification of RH for syngas production have been reported in the literature. Chen et al. (2015) studied the catalytic gasification of RH with five types of metal-oxide catalyst consisted of iron, cobalt, nickel, copper and zinc supported on γ-Al$_2$O$_3$, and reported that ZnO/γ-Al$_2$O$_3$ exhibited the highest activity and optimal conditions for syngas production were 800 °C, 0.1 MPa, 7.5% ZnO loading, 240 h^{-1} space velocity and 0.20-0.30 mm biomass particle size [10]. Zhang et al. investigated on how operating conditions affect the composition and distribution of gas products, and the composition of tar produced in the rice husk air-gasification using untreated and calcined dolomite as a catalyst [11]. Bharath et al. investigated the co-gasification in a bubbling fluidized bed gasifier of RH and coal and concluded that the addition of RH improved the total conversion of carbon, cold gas efficiency and syngas calorific value [12]. Makwana et al. optimized the reaction temperature for non-catalytic gasification of RH and reported the optimum temperature of 790 °C with a carbon conversion efficiency of 91.6%, the thermal efficiency of 75% and gas yield of 2.7 m^3/kg [13].

Zhao et al. researched the air gasification in a cyclone gasifier of RH to investigate how the equivalence ratio influences the temperature profiles, the composition of syngas, low heating value, tar content, total conversion of carbon and cold gas efficiency [14]. It was reported that air staged gasification with a secondary air ratio of 30% was able to produce syngas with reasonable heating value (4.72 MJ/Nm^3) and low tar content (1.85 g/Nm^3), respectively. Apart from these optimization studies, the gasification of RH has also been investigated in various other aspects. Simulation studies of gasification of RH have also been reported using computational fluid dynamics (CFD) models

to verify and predict the gasification behaviors [15], [16]. In terms of process development and economic feasibility of the gasification of RH, [17] and [18] had reported the exergy analysis and techno-economic analysis of RH gasification process. Alas, the application of chemometric modeling techniques such as artificial neuron principal component analysis (PCA) in identifying the correlation of response variables in gasification for syngas production is still lacking in literature [19], [20].

Hence, this study aims to investigate the significance of the parameters or response variables using various tools included TGA-MS, Fixed-batch Gasifier, and PCA. The effects of four parameters, which are reaction temperature, biomass particle size, catalyst loading and air to biomass ratio on the syngas composition from air gasification of rice husk are investigated using TGA-MS and reported. Besides, the optimum conditions of the air gasification obtained in the TGA-MS study were applied in a Fixed-batch gasifier to further confirm the catalytic effect of coal bottom ash (CBA) and to test the ability in a bench-scale application for future.

II. MATERIALS AND METHODS

A. Sample and Catalyst Preparation

The RH feedstock was gathered from a rice mill owned by BERNAS, Malaysia. The RH was sun-dried for a period of 36-48 h before it was pulverized to 250-1000 μm different particle sizes. The characteristics of RH were presented in Table 1.

TABLE I
PROXIMATE AND ULTIMATE ANALYSIS OF RICE HUSK

Characteristic	Weight percent (%)
Proximate analysis (dry basis)	
Moisture	5.56
Volatile matter	57.55
Ash	14.68
Fixed carbon (by difference)	22.21
Ultimate analysis (dry basis)	
C	38.47
H	5.75
S	<0.01
N	1.68
O (by difference)	54.09

The thermogravimetric analyzer EXSTAR TGA/DTA 6300 (Seiko Instrument Inc., Japan) was used to perform the proximate analysis in determining the ash content (AC), volatile matter (VM), and moisture content (MC). The weight percentage of the fixed carbon (FC) was calculated as in (1). Meanwhile, LECO CHNS-932 (LECO Corporation, USA) ultimate elemental analyzer was used to perform the ultimate analysis to understand the amount of elements C, H, N, O, and S in RH. This is a continuation study of previous literature in which the catalyst chosen was CBA [21]. The CBA was provided by a power plant owned by Tenaga Nasional Berhad (TNB) in Seri Manjung, Perak, Malaysia and it was sieved to <50 μm particle size to enhance the diffusion rate between reactant and catalysts.

$$FC\,(\%) = 100 - MC\,(\%) - VM\,(\%) - AC\,(\%) \qquad (1)$$

B. Experimental Procedure

1) TGA-MS Setup: The thermogravimetric analyzer (EXSTAR TG/DTA 6300) was used to carry out the gasification process and the composition of gas produced was assessed with a mass spectrometer connected. The RH sample and CBA catalyst were added into a ceramic crucible and inserted into the TGA equipment under N_2 environment according to the design array shown in Table 2.

TABLE II
DESIGN ARRAY WITH INPUT VARIABLES

Variable	Unit	Level			
		1	2	3	4
Reaction temperature	˚C	600	700	800	900
Particle size of RH	μm	250	500	750	1000
Amount of catalyst	wt%	2.5	5.0	7.5	10.0
Air to biomass ratio	-	1.00	1.25	1.50	1.75

The levels of the variables are determined based on the study by Shahbaz et al. (2017) [22]. A continuous nitrogen flow of 100 ml/min was introduced and kept for 10 mins at a temperature of 50 ˚C to purge the pyrolysis zone, preventing unwanted sample oxidation. Then, the air supplied as a gasifying agent was introduced into the system at a flow rate of 100 ml/min. All the samples were heated to the desired temperatures, as in Table 2, with 50 ˚C/min heating rate and kept constant for 10 mins to ensure the completion of the gasification process [23].

2) Fixed-batch Gasifier Setup: The catalytic in-situ gasification setup consists of an electrical vertical split tube furnace, gasifier unit and a liquid collecting unit. 10 g of RH along with the pre-determined CBA catalysts were mixed well and introduced into the gasifier unit. The thermocouple set was introduced into the gasifier to measure the reaction temperature. The gasifier unit is purged with a continuous flow of N_2 at 100 ml per min for 10 mins. Then, the air was supplied at 100 ml per min as a gasifying agent into the system at a flow rate of 100 ml/min [24]. The reactor was left to return to room temperature after the completion of the gasification, before performing the product analysis. The gaseous product was collected using a gasbag and analyzed through gas chromatography (Model: Clarus 500; Make: Perkin Elmer, USA) coupled with flame ionization detector (FID).

C. Principal Component Analysis

Principal component analysis (PCA) is an analytical method that is designed for multivariate structure analysis [24]. It can shrink the sizes of a huge data set which consists of a large number of correlated variables while maintaining minimal data loss [25]. This can be achieved by transforming the corresponding initial variables into a new set of non-related variables which are noted as principal components (PC). It is commonly used to investigate the degree of influences of the manipulated variables on the responding variables [26], [27]. In this work, PCA is applied to determine the influence of various operating parameters, including those in Table 2, on the product gas composition.

In obtaining PCs, the eigenvector-eigenvalue problem as in (2) is used, where C refers to the correlation matrix that encompasses the correlation between each variable, as in (3),

while v and λ refer to the eigenvector and eigenvalue respectively. It is worthy to note that the largest λ always corresponded to the first PC (or PC1), followed by the PC2, and so on. This indicates that PC1 holds most of the total data variance followed by PC2, and so forth [26]. VAR_a and VAR_b denote the comparative variables a and b, respectively. $\overline{VAR_a}$ and $\overline{VAR_b}$ are the mean of the respective variables, while the standard deviation of these variables are noted as σ_{VARa} and σ_{VARb}.

$$C_V = \lambda \, v \qquad (2)$$

$$Correlation(VAR_a, VAR_b) = \frac{1}{n-1}\sum_1^n \left(\frac{VAR_a - \overline{VAR_a}}{\sigma_{VAR_a}}\right)\left(\frac{VAR_b - \overline{VAR_b}}{\sigma_{VAR_b}}\right) \qquad (3)$$

In order to obtain sufficient data significance and minimal data loss, a screen plot method with a threshold cut (i.e., minimum cumulative variance) of 90 % is opted [27]. It is expressed as in (4). The data set can now be transformed into new factor score set by using (5), where S refers to the normalized data matrix. Note that in this matrix, the original data is normalized to the standard score.

$$Cumulative \; Variance \geq 90 \; \% \qquad (4)$$

$$Factor \; Score = S \, v \qquad (5)$$

Since PCs consist of convex combinations among initial variables, it is necessary to quantify the loading between initial variables and PCs, as well as their respective contribution rate, via (6) and (7) respectively. Y refers to the projection matrix, and e denotes the eigenvector assigned to each PC. In general, the variable that contributes the most is the most influencing variable to that PC [28].

$$\mathbf{Y} = \sqrt{\lambda} \cdot \mathbf{v} \qquad (6)$$

$$Contribution = |e| \, / \, \Sigma|e| \; x \; 100 \qquad (7)$$

III. RESULTS AND DISCUSSION

A. Effect of Different Reaction Temperature

Fig. 1 illustrates the results of effect of reaction temperature. It is found that the H_2 composition rises with temperature, from 17.2 to 28.2 vol%. As predicted, the rising temperature lead to a higher gas yield, and a lesser tar and solid residues, which possibly caused by the further cracking of liquids and char with the gasifying medium. The rise in syngas composition from 67.2 to 73.8 vol% at temperature from 600 to 900 ˚C can be explained through several reasons like larger production of gaseous in initial gasification step with faster rate at high temperature or the evolution of gaseous through endothermal char gasification reaction is highly favorable to higher temperature [28]. The temperature elevation was found to promote the H_2 formation with a significant decrease of CH_4 from 16.4 to 7.1 vol%. The endothermic reactions of dry reforming of hydrocarbon (R1), methanations (R2-3), water gas reactions (R4-5) and water

gas shift reaction (R6) showed a positive result in the syngas composition with increasing temperature, in align with the Le-Chatelier's principle.
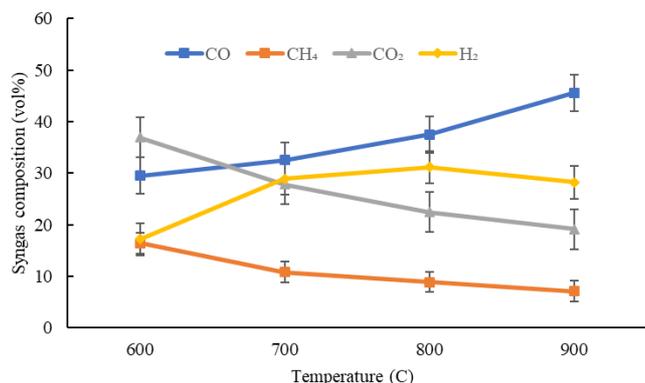
Fig. 1 Effect of reaction temperature on gas composition (Reaction condition: particle size of biomass = 250 µm, amount of catalyst = 10 wt% and air to biomass ratio = 1.25)

Besides, R6 commonly present in gasification process when there is presence of water vapor in air. This creates a homogeneous phase to promote the H_2 yield by reacting the CO_2 produced [29]. This statement was supported with the change in composition of CO_2, in which when temperature elevated from 600 to 900 °C the CO_2 decreased from 36.9 to 19.1 vol%.

$$CH_4 + CO_2 \leftrightarrow 2CO + 2H_2 \tag{R1}$$

$$CH_4 + H_2O \leftrightarrow CO + 3H_2 \tag{R2}$$

$$CO_2 + 4H_2 \leftrightarrow CH_4 + 2H_2O \tag{R3}$$

$$C + H_2O \leftrightarrow CO + H_2 \tag{R4}$$

$$C + 2H_2O \leftrightarrow CO_2 + 2H_2 \tag{R5}$$

$$CO + H_2O \leftrightarrow CO_2 + H_2 \tag{R6}$$
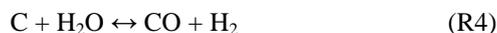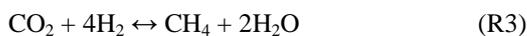
B. *Effect of Different Particle Size of Biomass*

Fig. 2 illustrates the syngas composition performance for RH at different particle size as in Table 2.
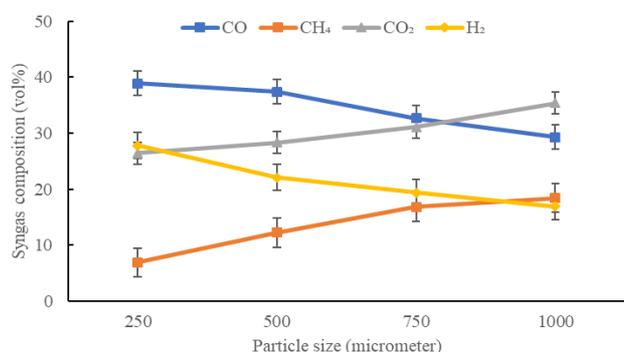
Fig. 2 Effect of particle size of RH on gas composition (Reaction condition: reaction temperature: 900 °C, amount of catalyst = 10 wt% and air to biomass ratio = 1.25)

It is found that the syngas production clearly increased with decreased particle size. This trend can be explained through mass transfer and diffusion study. With increasing particle size comes with increasing mass diffusion resistances, thus it is harder for the produced gases to diffuse out from inside the particle. It is also noted that with larger particle size, the smaller is the total surface area available for the gasification to occur, which also contributed on the decreasing syngas production at larger particle size. Moreover, large particles are difficult to be captured by fluidizing gas and thus, the reactions such as dry reforming of hydrocarbon and methanation take longer time to be achieved [30].

C. *Effect of Amount of Catalyst on Syngas Composition*

Fig. 3 illustrates the effect of amount of catalyst on syngas production.
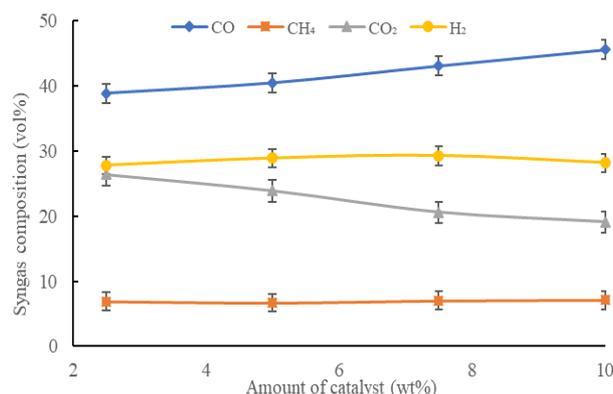
Fig. 3 Effect of amount of catalyst on gas composition (Reaction condition: reaction temperature: 900 °C, particle size of RH = 250 µm and air to biomass ratio = 1.25)

It can be seen that the amount of catalyst is directly proportional to the syngas composition. As the amount of catalyst increased from 2.5 to 10 wt%, the syngas composition also increased from 66.7 to 73.8 vol%, but the CO2 composition had reduced from 26.4 to 19.1 vol%. This improved the syngas production, resembling impregnated metal catalysts. In a similar study, Chen et al. (2016) has found that the concentration of CO2 is reduced but concentration of H2 is increased with the CaO impregnation in Fe/CaO catalyst via reduction and carbonation reactions (R7-8) [31]. The symbol "Me" in R7 refers to metal elements. This phenomenon is seen in this study, where the concentration of CO2 was decreases up to 7.3 vol% when the amount of catalyst raised from 2.5 to 10 wt%.

Furthermore, the increasing CO concentration (up to 6.7 vol%) and the decreased in CO_2 as the amount of catalyst in CBA increased can be due to the Boudourad reaction as shown in R9. Moreover, it can be observed that the CH_4 composition was almost similar regardless the addition of catalyst. Similar observation has been reported in previous study, in which catalyst has less attributed to the conversion of CH_4 [32].

$$nH_2 + Me_mO_n \leftrightarrow mMe + nH_2O \tag{R7}$$

$$CaO + CO_2 \rightarrow CaCO_3 \tag{R8}$$

$$CO_2 + C \leftrightarrow 2CO \tag{R9}$$
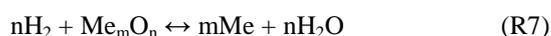
D. Effect of Air to Biomass Ratio on Syngas Composition

Fig. 4 demonstrates how the ratio of air to biomass affects syngas composition in gasification.
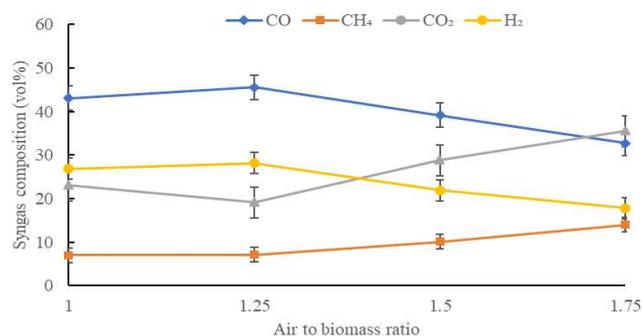
Fig. 4 Effect of air to biomass ratio on gas composition (Reaction condition: reaction temperature: 900 ˚C, particle size of RH = 250 µm and amount of catalyst= 10 wt%)

The oxygen content in the air is approximately 21 %. Two trends can be observed in Fig. 4, in which H_2 and CO content firstly increased and then followed by decrement as air to biomass ratio increased. Similar trend is reported in previous study when they studied the H_2 production performance from air gasification of agriculture waste [33]. The air to biomass ratio is not only portrays the quantity of oxygen inserted to the gasifier but also plays a role in the gasification temperature under auto thermal operation condition. The higher the air to biomass ratio means the higher the gasification temperature, in which the gasification process is accelerated due to increased oxygen content, subsequently enhance the purity of the product to a certain extend [33]. Thus, two opposing factors of air to biomass ratio are both influencing the composition of the gas. The results showed that as the air to biomass ratio increased from 1 to 1.25, more heat is released to enhance the tar cracking secondary reaction, resulting in increasing H_2 and CO. However, excess of air as gasifying agent would promote the oxidation of CO to CO_2. Therefore, the CO_2 composition increased associated with a significant dropped in CO composition. Furthermore, the CH_4 had shown significant increasing trend due to intensification of the CH_4 combustion; in which large number of gaseous and combustion reactions retards methanation reaction.

E. Syngas Compositions Obtained Using Fixed Bed Reactor

Fig. 5 shows the comparative results of gaseous products obtained from TGA-MS and fixed bed reactor. The syngas composition obtained in catalytic air gasification using the fixed bed reactor was 3.25 % higher than TGA-MS. Besides, the solid, liquid, and gaseous yields obtained using the fixed bed reactor were 6.2 wt%, 9.7 wt% and 84.1 wt%, respectively. Table 3 shows that CBA is a potential candidate for replacing the commercial catalysts in catalytic gasification process. For instance, the syngas composition

obtained in the present study using CBA as catalyst is 8.18% higher than previous literature reported [34].
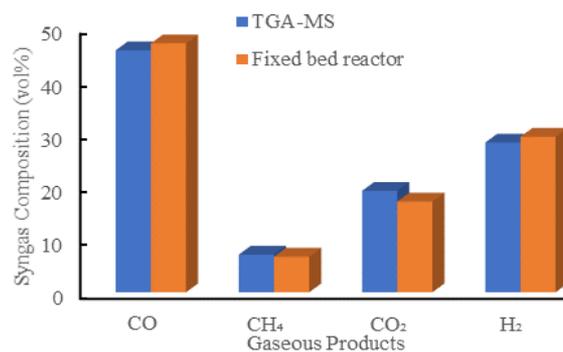
Fig. 5 Gaseous products obtained from TGA-MS and Fixed bed reactor.

F. Principal Component Analysis Results

The computed PC has been applied on the sample description shown in Table 4, and the screen plot is generated as shown in Fig. 6.
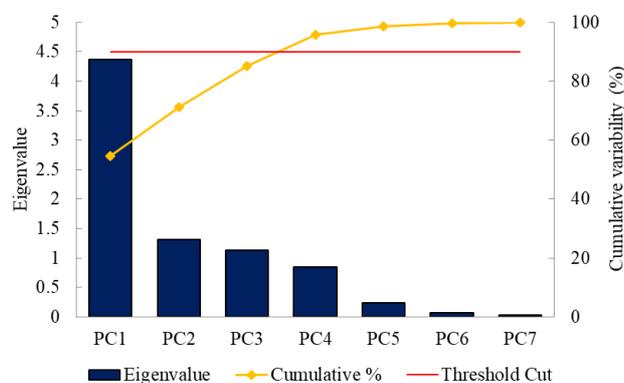
Fig. 6 Screen plot of principal components

The PCs are sorted by descending eigenvalue, and then the cumulative eigenvalue (also cumulative variance) is plotted. From the figure, it is clearly seen that there is a significant drop of eigenvalue between PC1 and PC2. This indicates that the first PC has highest influences on the initial data set. However, Fig. 6 shows that the criteria of having 90% minimum cumulative variance can only be achieved if the first four PCs are considered. Therefore, four PCs are satisfactory for this work.

This contradiction is mainly due to the variation of each parameter, further validated by the contribution chart in Fig. 7. From the figure, it shows that all the corresponding variables contribute significantly in PC1, while its contribution on other PCs is very insignificant (< 5%). From PC2 onwards, the PCs are mainly contributed by the variation on the input parameters (i.e., temperature, biomass particle size, catalyst loading and air-to-biomass ratio). In other words, this further confirm the former assumption. Thus, PC1 is the critical PC that required further analysis.

1788

Optimum conditions	Catalyst	Gasifying agent	Findings	Reference
Temperature: 800 °C Pressure: 0.1 MPa Catalyst loading: 7.5% Space velocity: 240 h^{-1} Particle size: 0.20-0.30 mm	$ZnO/\gamma-Al_2O_3$	CO_2	CO content: 22.1wt%	[10]
Temperature: 790 °C Particle size: width = 0.8-1 mm, length = 3-5 mm Biomass feed rate: 30-32 kg/h Air flow rate: 43.0 m^3/h Stoichiometric ratio: 0.3	-	Air	H$_2$ content: 14wt% CO content: 7wt% Gas yield: 1.8-2.7 Nm^3/kg	[13]
Temperature: 900 °C Biomass feed: 50g	Ni/RHC	-	H$_2$ + CO content: 69.96 wt% Gas yield: 53.9 wt%	[34]
Temperature: 800 °C Steam/biomass ratio: 1.33 Equivalence ratio: 0.22	nano-NiO/γ-Al$_2$O$_3$	Air-steam	H$_2$ content: 48.7wt% CO content: 25.2wt% Gas yield: 2.35 Nm^3/kg	[35]
Temperature: 900 °C Air/biomass ratio: 1.25, Particle size <250 µm	Coal bottom ash	Air	H$_2$ content: 48.7wt% CO content: 25.2 % Gas yield: 84.1 wt%	Present work

TABLE IV
SAMPLE DESCRIPTION OF THE RESULTS.

Sample ID	Parameters					Syngas Composition (%)			
	Temperature (°C)	Particle Size (mm)	Catalyst Load (%wt)	Air to biomass ratio		CO	CH$_4$	CO$_2$	H$_2$
S1	600	250	10.0	1.25		29.5	16.4	36.9	17.2
S2	700	250	10.0	1.25		32.5	10.8	27.8	28.9
S3	800	250	10.0	1.25		37.5	8.9	22.4	31.2
S4	900	250	10.0	1.25		45.6	7.1	19.1	28.2
S5	900	1000	10.0	1.25		29.3	18.4	35.4	16.9
S6	900	750	10.0	1.25		32.7	16.8	31.1	19.4
S7	900	500	10.0	1.25		37.4	12.2	28.3	22.1
S8	900	250	2.5	1.25		38.9	6.9	26.4	27.8
S9	900	250	5.0	1.25		40.5	6.7	23.9	28.9
S10	900	250	7.5	1.25		43.7	6.4	20.6	29.3
S11	900	250	10.0	1.00		43.1	7.0	23.0	26.9
S12	900	250	10.0	1.50		39.2	10.1	28.8	21.9
S13	900	250	10.0	1.75		32.7	14.0	35.5	17.8
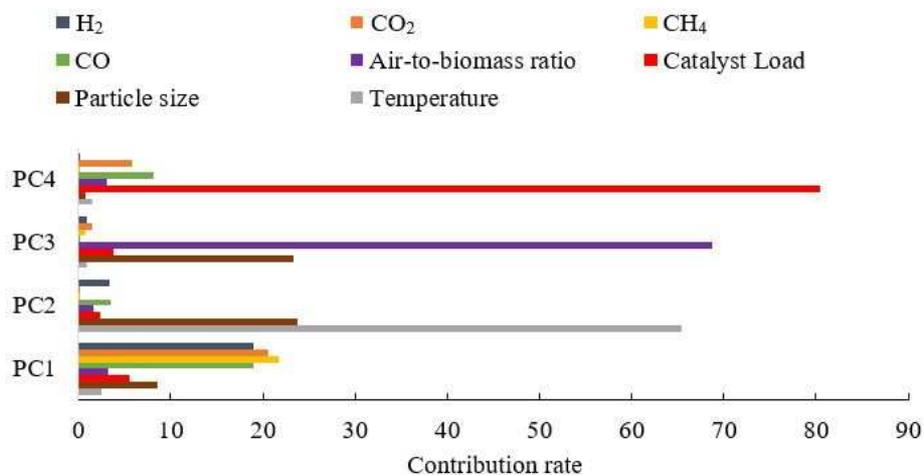
Fig. 7 Contribution rate of each variable on the PCs.

From the factor score diagram as shown in Fig. 8, it can be clearly seen that samples S4, S8, S9 and S10 are all clustered together.
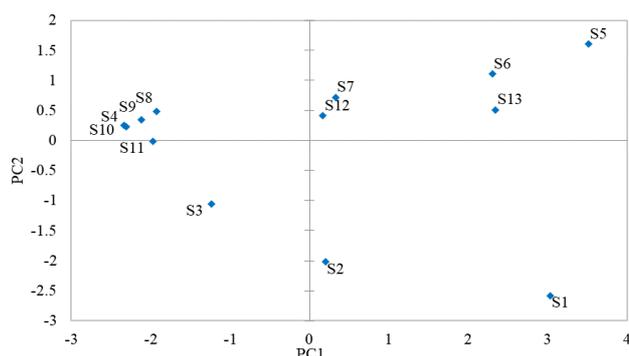
Fig. 8 Factor scores for each sample.

This indicates that the effect of using different catalyst loading is comparatively insignificant as compared to other parameters, as only catalyst loading is differed between those samples. It can also be seen through Fig. 8, as the contribution rate of catalyst loading on PC1 up to PC3 is very insignificant (< 6 %).
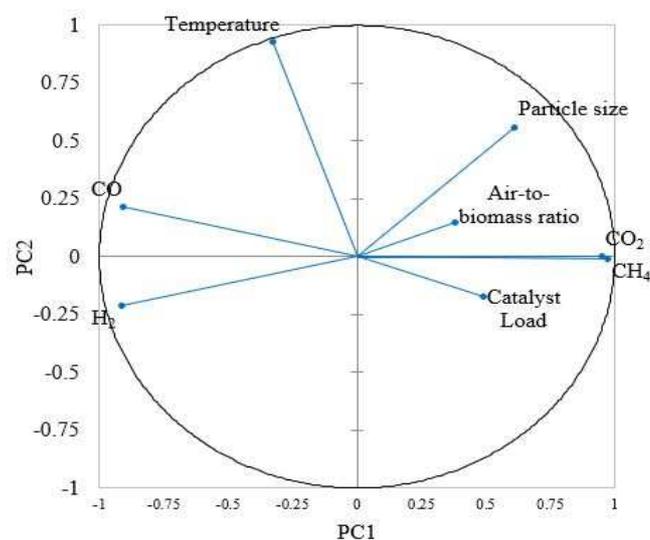
Fig. 9 Loading plot of PCA.

Based on the loading plot as given in Fig. 9, temperature is positively proportional toward H_2 and CO composition, while negatively with CO_2 and CH_4. Contrarily, particle size, air-to-biomass ratio and catalyst loading have a positive relationship with CO_2 and CH_4 but negative with H_2 and CO. Note that the drawback of PCA is that it is unable to capture the non-linear behavior of the performance. However, this issue can be addressed by having appropriate study range of each operating parameter.

IV. CONCLUSION

The process optimization study of catalytic gasification was successfully conducted in the TGA-MS system with coal bottom ash as catalyst. It was found out that the optimum input parameters for syngas composition were at reaction temperature of 900 ˚C, RH particle size of 250 μm,

10 wt% of amounts of catalyst and 1.25 air to biomass ratio to obtain 73.8 vol% of syngas. The optimum conditions of the air gasification obtained in the TGA-MS study was also applied in a fixed bed gasifier to confirm the influences of coal bottom ash as catalyst further. It showed that the syngas composition obtained using fixed bed reactor was 3.25 % higher than TGA-MS (76.2 vol%). From the PCA analysis, it showed that reaction temperature is the dominant factor in enhancing the syngas composition and catalyst loading is the most insignificant factor in producing the syngas.

REFERENCES

[1] G. B. Upton and B. F. Snyder, "Funding renewable energy: An analysis of renewable portfolio standards," Energy Economics, vol. 66, pp. 205-216, Aug. 2017.

[2] P. Faúndez, "Renewable energy in the equilibrium mix of electricity supply sources," Energy Economics, vol. 67, pp. 28-34, Sep. 2017.

[3] S. B. Tsai, Y. Xue, J. Zhang, Q. Chen, Y. Liu, J. Zhou, and W. Dong, "Models for forecasting growth trends in renewable energy," Renewable and Sustainable Energy Reviews, vol. 77, pp. 1169-1178, Sep. 2017.

[4] M. Ozturk, N. Saba, V. Altay, R. Iqbal, K. R. Hakeem, M. Jawaid, and F. H. Ibrahim, "Biomass and bioenergy: An overview of the development potential in Turkey and Malaysia," Renewable and Sustainable Energy Reviews, vol. 79, pp. 1285-1302, Nov 2017.

[5] H. L. Zhu, Y. S. Zhang, M. Materazzi, G. Aranda, D. J. L. Brett, P. R. Shearing, and G. Manos, "Co-gasification of beech-wood and polyethylene in a fluidized-bed reactor," Fuel Processing Technology, vol. 190, pp. 29-37, Jul. 2019.

[6] D.T. Pio, L. A. C. Tarelho, R. G. Pinto, M. A. A. Matos, J. R. Frade, A. Yaremchenko, G. S. Mishra, and P. C. R. Pinto, "Low-cost catalysts for in-situ improvement of producer gas quality during direct gasification of biomass," Energy, vol. 165, pp. 442-454, Dec. 2018.

[7] F. Pinto, R. André, M. Miranda, D. Neves, F. Varela, and J. Santos, "Effect of gasification agent on co-gasification of rice production wastes mixtures," Fuel, vol. 180, pp. 407-416, Sep. 2016.

[8] G. Oh, H. W. Ra, S. M. Yoon, T. Y. Mun, M. W. Seo, J. G. Lee, and S. J. Yoon, "Gasification of coal water mixture in an entrained-flow gasifier: Effect of air and oxygen mixing ratio," Applied Thermal Engineering, vol. 129, pp. 657-664, Jan. 2018.

[9] H. Weldekidan, V. Strezov, G. Town, and T. Kan, "Production and analysis of fuels and chemicals obtained from rice husk pyrolysis with concentrated solar radiation," Fuel, vol. 233, pp. 396-403, Dec. 2018.

[10] Z. M. Chen and L. Zhang, "Catalyst and process parameters for the gasification of rice husk with pure CO2 to produce CO," Fuel Processing Technology, vol. 133, pp. 227-231, May 2015.

[11] G. Zhang, H. Liu, J. Wang, and B. Wu, "Catalytic gasification characteristics of rice husk with calcined dolomite," Energy, vol. 165, pp. 1173-1177, Dec. 2018.

[12] M. Bharath, V. Raghavan, B. V. S. S. S. Prasad, and S. R. Chakravarthy, "Co-gasification of Indian rice husk and Indian coal with high-ash in bubbling fluidized bed gasification reactor," Applied Thermal Engineering, vol. 137, pp. 608-615, Jun. 2018.

[13] J. P. Makwana, J. Pandey, and G. Mishra, "Improving the properties of producer gas using high temperature gasification of rice husk in a

pilot scale fluidized bed gasifier (FBG)," Renewable Energy, vol. 130, pp. 943-951, Jan. 2019.

[14] Y. Zhao, S. Sun, H. Che, Y. Guo, and C. Gao, "Characteristics of cyclone gasification of rice husk," International Journal of Hydrogen Energy, vol. 37, pp. 16962-16966, Nov. 2012.

[15] J. J. R. Behainne and J. D. Martinez, "Performance analysis of an air-blown pilot fluidized bed gasifier for rice husk," Energy for Sustainable Development, vol. 18, pp. 75-82, Feb. 2014.

[16] X. Gao, F. Xu, F. Bao, C. Tu, Y. Zhang, Y. Wang, Y. Yang, and B. Li, "Simulation and optimization of rice husk gasification using intrinsic reaction rate based CFD model," Renewable Energy, vol. 139, pp. 611-620, Aug 2019.

[17] P. C. Murugan and S. J. Sekhar, "Species – Transport CFD model for the gasification of rice husk (Oryza Sativa) using downdraft gasifier, Computers and Electronics in Agriculture, vol. 139, pp. 33-40, Jun. 2017.

[18] K. Manatura, J. H. Lu, K. T. Wu, and H. T. Hsu, "Exergy analysis on torrefied rice husk pellet in fluidized bed gasification," Applied Thermal Engineering, vol. 111, pp. 1016-1024, Jan 2017.

[19] P.W. Olupot, A. Candia, E. Menya, and R. Walozi, "Characterization of rice husk varieties in Uganda for biofuels and their techno-economic feasibility in gasification," Chemical Engineering Research and Design, vol. 107, pp. 63-72, Mar. 2016.

[20] M. Buyukada, "Probabilistic uncertainty analysis based on Monte Carlo simulations of co-combustion of hazelnut hull and coal blends: Data-driven modeling and response surface optimization," Bioresource Technology, vol. 225, pp. 106-112, Feb. 2017.

[21] A. C. M. Loy, S. Yusup, B. L. F. Chin, D. K. W. Gan, M. Shahbaz, M. N. Acda, P. Unrean, and E. Rianawati, "Comparative study of in-situ catalytic pyrolysis of rice husk for syngas production: Kinetics modelling and product gas analysis," Journal of Cleaner Production, vol. 197, pp. 1231-1243, Oct. 2018.

[22] M, Shahbaz, S. Yusup, A. Inayat, D. O. Patrick, A. Pratama, and M. Ammar, "Optimization of hydrogen and syngas production from PKS gasification by using coal bottom ash," Bioresource technology, vol. 241, pp. 284-295, Oct. 2017.

[23] A. C. M. Loy, S. Yusup, M. K. Lam, B. L. F. Chin, M. Shahbaz, A. Yamamoto, and M. N. Acda, "The effect of industrial waste coal bottom ash as catalyst in catalytic pyrolysis of rice husk for syngas production," Energy Conversion and Management, vol. 165, pp. 541-554, Jun. 2018.

[24] Y. Chen and Y. Hao, "Integrating principle component analysis and weighted support vector machine for stock trading signals prediction," Neurocomputing, vo. 321, pp. 381-402, Dec. 2018.

[25] S. Hosseinpour, M. Aghbashlo, and M. Tabatabaei, "Biomass higher heating value (HHV) modeling on the basis of proximate analysis using iterative network-based fuzzy partial least squares coupled with principle component analysis (PCA-INFPLS)," Fuel, vol. 222, pp. 1-10, Jun. 2018.

[26] A. C. M. Loy, D. K. W. Gan, S. Yusup, B. L. F. Chin, M. K. Lam, M. Shahbaz, and E. Rianawati, "Thermogravimetric kinetic modelling of in-situ catalytic pyrolytic conversion of rice husk to bioenergy using rice hull ash catalyst," Bioresource Technology, vol. 261, pp. 213-222, Aug. 2018.

[27] B. S. How and H. L. Lam, "Sustainability evaluation for biomass supply chain synthesis: Novel principal component analysis (PCA) aided optimisation approach," Journal of Cleaner Production, vol. 189, pp. 941-961, Jul. 2018.

[28] R. M. Esfahani, W. A. Wan Ab Karim Ghani, M. A. Mohd Salleh, and S. Ali, "Hydrogen Rich Gas Production from Palm Kernel Shell by Applying Air Gasification in Fluidized Bed Reactor," Energy & Fuels, vol. 26, pp. 1185-1191, Feb 2012.

[29] R. Moreira, A. Moral, F. Bimbela, A. Portugal, A. Ferreira, J. L.Sanchez, and L. Gandía, "Syngas production via catalytic oxidative steam reforming of glycerol using a Co/Al coprecipitated catalyst and different bed fillers," Fuel Processing Technology, vol. 189, pp.120-133, Jun. 2019.

[30] D. Y. C. Leung and C. L. Wang, "Kinetic Modeling of Scrap Tire Pyrolysis," Energy & Fuels, vol. 13.2, pp. 421-427, Mar. 1999.

[31] S. Yang, X. Zhang, L. Chen, L. Sun, X. Xie, and B. Zhao, "Production of syngas from pyrolysis of biomass using Fe/CaO catalysts: Effect of operating conditions on the process," Journal of Analytical and Applied Pyrolysis, vol. 125, pp. 1-8, May 2017.

[32] S. A. Sulaiman, R. Roslan, M. Inayat, and M. Yasin Naz, "Effect of blending ratio and catalyst loading on co-gasification of wood chips and coconut waste," Journal of the Energy Institute, vol. 91, pp. 779-785, Oct. 2018.

[33] W. A. Wan Ab Karim Ghani, R. A. Moghadam, M. A. M. Salleh, and A. B. Alias, "Air gasification of agricultural waste in a fluidized bed gasifier: hydrogen production performance," Energies, vol. 2, pp. 258-268, Jun. 2009.

[34] S. Zhang, Q. Dong, L. Zhang, and Y. Xiong, "High quality syngas production from microwave pyrolysis of rice husk with char-supported metallic catalysts," Bioresource Technology, vol. 191, pp. 17-23, Sep. 2015.

[35] J. Li, J. Liu, S. Liao, and R. Yan, "Hydrogen-rich gas production by air-steam gasification of rice husk using supported nano-NiO/γ-Al2O3 catalyst," International Journal of Hydrogen Energy, vol. 35, pp. 7399-7404, Jul. 2010.